Effects Of Unbalanced Magnetic Force And Torque Ripple On The Performance Of A Double Stator Permanent Magnet Machine

Chukwuemeka C. AWAH[1] ⓘ, Stephen E. OTI[2] ⓘ, Ifeanyi K. NNABUENYI[3]

[1]Electrical and Electronic Engineering, Michael Okpara University of Agriculture, Umudike, Umuahia, Abia State, Nigeria
[2]Electrical Engineering, University of Nigeria, Nsukka, Enugu State, Nigeria
[3]Instrument QA/QC Arco M&E, NLNG Sub Contractor, Bonny, Rivers State, Nigeria

ccawah@ieee.org, stephen.oti@unn.edu.ng, ifeanyiknnabuenyi@gmail.com

Abstract. *The effect of unbalanced magnetic force and torque ripple of on the output performance of a double stator switched-flux permanent magnet machine would be investigated and compared, with particular reference to the machine's varying rotor pole number. The finite element analysis (FEA) predicted machine parameters are: unbalanced magnetic force (UMF), total harmonic distortion (THD), torque ripple (Tr), cogging torque and static torque. The considered machine types having 10-, 11-, 13- and 14-rotor pole numbers are designated as: 6S/10P, 6S/11P, 6S/13P and 6S/14P, respectively; 6S represents six (6) stator slot or teeth number. It is revealed that the machine types that have odd number of rotor poles would have lower machine output characteristics such as: low cogging torque, low torque ripple and low total harmonic distortion of the voltage, compared to the ones that have even number of rotor poles; though, with higher amount of unbalanced magnetic force on the rotor. Further, the sensitivity of the machine's output performances due to electric loadings is higher than its corresponding response as a result of machine's varying rotational speed. More so, the machine types having odd number of rotor poles would have higher air gap flux density magnitudes; and would also exhibit better average torque per magnet usage, which is desirable for reduced cost implications.*

Keywords

Cogging torque, torque ripple, total harmonic distortion, unbalanced magnetic force.

1. Introduction

Output characteristics such as: unbalanced magnetic force (UMF), total harmonic distortion (THD), cogging torque, torque ripple (Tr) or torque pulsations, etc. of an electrical machine are inimical to good electromagnetic performance of the machine. Hence, the magnitudes of these machine output characteristics are numerically estimated in this study, using finite element analysis (FEA) procedure; in order to evaluate its overall impact on the machine output performance(s) and proffer prospects for its consequent reductions through further researches.

The winding factor geometric level of an electric machine which invariably gives rise to its electromotive force and electromagnetic torque amplitudes are functions of pole numbers and winding configurations [1]. Hence, to a large extent the output performance(s) of a given electric machine would depend upon its number of rotor poles, and thus the resulting winding factors. It is noted that undesirable machine parameters such as torque pulsations, UMF, noise, vibration and reduced machine efficiency are larger in machines that are equipped with single-tooth winding plan compared to the ones that have distributed windings; though, with reduced cost effect. Nevertheless, the single-tooth winding machine types are usually preferred in flux-weakening and fault-tolerance applications, due to their good inductance features. It is important to note that single-tooth non-overlapping winding topology is adopted in this present study.

It is further highlighted in [2] that the output of parameters such as torque ripple and efficiency of a given electrical machine would be greatly influenced by its pole and slot number arrangement. Also, the percentage of torque ripple in a given electrical machine could be heightened due to the impact of armature reaction; particularly, during electric overload [3].

Furthermore, unbalanced magnetic force (UMF) in a given electrical machine would be worsened if the machine is associated with any sort of eccentricity defect [4] and this deteriorated condition could result to machine failure or collapse, as opined in [5]. The resultant UMF magnitude would also depend on pole alignment of the machine with the magnetic fields. More so, higher UMF effect would be experienced in the machine if, low energy density and thinner magnets are employed. Similarly, the magnitudes of both the UMF and cogging torque of an electric machine would be increased, owing to irregular magnetization fields as well as unevenness influence of the rotor periphery, as established in [6]. It is observed in [6] that the magnitudes of cogging torque and UMF would be a function of the difference between the machine's slot and rotor pole numbers; the greater this difference, the better for the machine's effectiveness.

Moreover, it is established in [7] that the number of rotor poles could significantly affect the resulting UMF amplitude of an electric machine, even without the presence of eccentricity. Similarly, high UMF value could consequently reduce the average torque of a given electrical machine. Meanwhile, a standard UMF index measuring criteria is developed in [8] using the machine's structural geometric variables and performance metrics, in order to estimate and compare the UMF levels of different kinds of machine. Thus, such criteria would serve as guides to operate electrical machines within an acceptable UMF limits.

Furthermore, the impact of pole number on other unwanted machine outputs such as no-load or cogging torque and on-load voltage distortions of permanent magnet machines are demonstrated in [9] and [10] with valid test results. The results in [9] and [10] reveal that amongst other machine variables like the operating frequency and architectural plan of the machine, the rotor and stator pole arrangements play significant roles in determining the magnitude of both the cogging torque and voltage distortions in such machines. Additionally, the class of machine, based on the machine's stator pole-pitch ratio is also used as a good benchmark to measure the resulting amplitudes of cogging torque and voltage distortion in the machine. Nevertheless, considerable reduction on these undesirable machine inabilities could be achieved in a given electrical machine, by deploying the tooth-shifting strategy, as discussed in [11] or through appropriate rotor skewing approach [12].
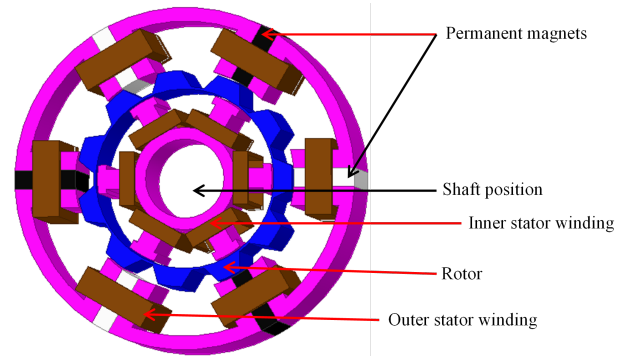

Fig. 1: The investigated machine three-dimensional structural plan, 11 poles [21].

Again, it is important to note that large amounts of UMF and cogging torque in an electrical machine could be so disastrous to the extent of degenerating into noise and vibration formation in the system, as highlighted in [13] and [14]. However, these unattractive machine features are mainly attributed to low order harmonic components. In addition, cogging torque value of an electrical machine could trigger its torque ripple influence. It is demonstrated in [15] and [16] that slot number and pole number of any given electric machine are vital in deciding the amount of torque ripple in the machine; also, a relationship exists between these pole and slot numbers and its consequent harmonic elements.

More so, torque ripple value of a double stator permanent magnet machine having multi-excitation scheme could be lessened, by implementing a counteracting low energy density magnet in the system and concurrently minimize the harmonic distortion effects from the other excitation sources [17]. Meanwhile, machine configurations that have low voltage THD would naturally yield a corresponding low cogging torque value, as inferred from [18].

A quantitative comparison of the effect of rotor pole number on some unwanted machine features such as: unbalanced magnetic force, cogging torque, torque ripple and total harmonic distortion is studied and presented in this current investigation, in order to have an estimated magnitude of these effects on the overall performance of a given double stator permanent magnet machine; and thus, to suggest possible reduction strategies of such undesirable machine characteristics, in further investigation(s).

2. Methodology

The investigated machine model having 11-pole number is shown in Fig. 1; while the magnetic-field vector outlines of all the compared machine topologies are displayed in Fig. 2. The implemented software in this study is ANSYS/MAXWELL-2D software, ver-
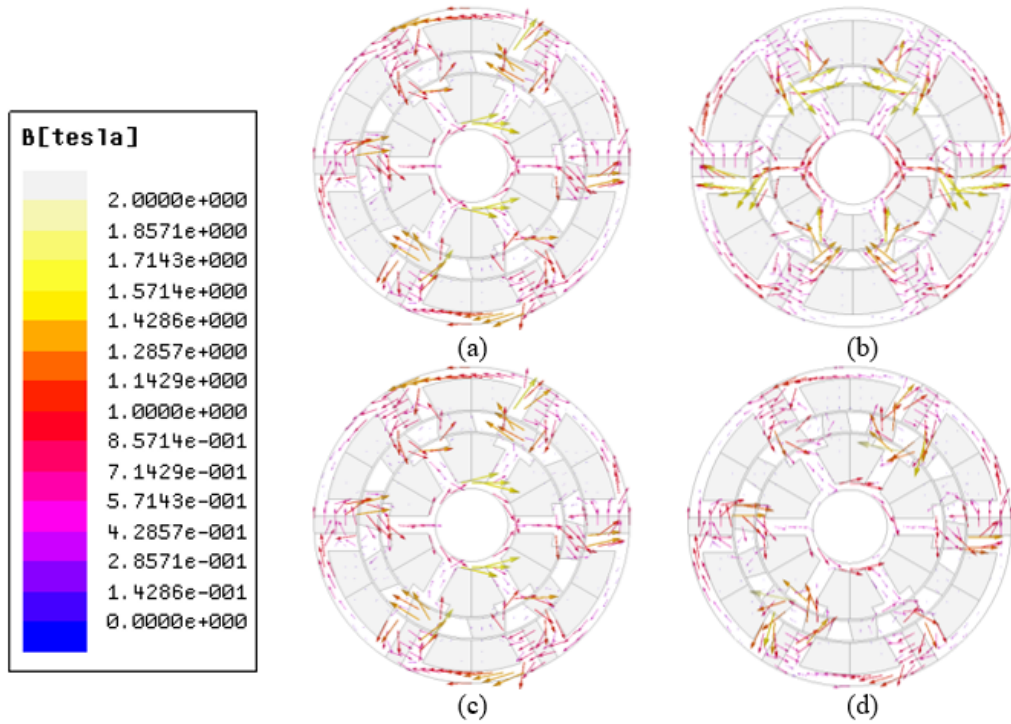
Fig. 2: Magnetic field vector outlines (a) 6S/10P, (b) 6S/11P, (c) 6S/13P and (d) 6S/14P.

sion 15.0. Additionally, MATLAB software is also implemented. It is obvious from Fig. 2 that magnetic fields would move from both the inner and outer excitation stators toward the air gap, for a consequent electromagnetic energy conversion process, in order to yield the required electromotive force, electromagnetic torque and output power. The investigated machine types having 10-, 11-, 13- and 14-rotor pole numbers are designated as: 6S/10P, 6S/11P, 6S/13P and 6S/14P, respectively. Note that 6S signifies six (6) stator teeth number of both the inner and outer stators while P represents the rotor poles. The studied machine belongs to flux-switching permanent magnet (FSPM) machine category. The feasible stator teeth (pole) and rotor pole number combinations of FSPM machine is mathematically stated in Eq. (1) and Eq. (2). Thus, a three-phase twelve-rotor pole (12P) configuration is not a possible combination in FSPM machine topologies. Therefore, a 12P rotor pole structure of an FSPM machine is only practicable in a single-phase configuration, as detailed in [19]. More so, the stator teeth number of any given FSPM machine is always a multiple of six (6). It is important to note that the number of rotor poles of any given FSPM machine is equivalent to the pole pairs of other conventional electric machines [20].

where N_s and N_r are the stator and rotor poles, m is the number of phases, k_1 is an integer and should be an even number when m is an odd number [20].

Eq. (3) is the mathematical expression of the estimated total harmonic distortion (THD) in this study, as demonstrated in [22]. Also, the horizontal and vertical components of UMF in a given electric machine could be estimated using Eq. (4) and Eq. (5), respectively. It is worth noting that unbalanced magnetic force (UMF) is often referred to as unbalanced magnetic pull (UMP). Similarly, the predicted FEA cogging torque cycles per electric revolution of the compared machines (n) is given in Eq. (6). Hence, the mathematical expression would result to 3 and 6 cycles, for the considered even and odd number of rotor poles, respectively.

$$THD = \frac{\sqrt{E_2^2 + E_3^2 + ... + E_n^2}}{E_1}, \qquad (3)$$

where E_1 is the fundamental magnitude of the induced electromotive force, $E_2, ..., E_n$ are the sub-harmonic voltages, adopted n^{th} order = 59.

$$F_x = \int_0^{2\pi} \frac{B_r^2}{2\mu_0} \frac{D}{2} l \cos\theta_s d\theta_s, \qquad (4)$$

$$F_y = \int_0^{2\pi} \frac{B_r^2}{2\mu_0} \frac{D}{2} l \sin\theta_s d\theta_s, \qquad (5)$$

where B_r is the flux density in the radial direction, D is the stator inner diameter, l is the axial length of the

$$N_s = k_1 m, \quad k_1 = 1, 2, ..., \qquad (1)$$
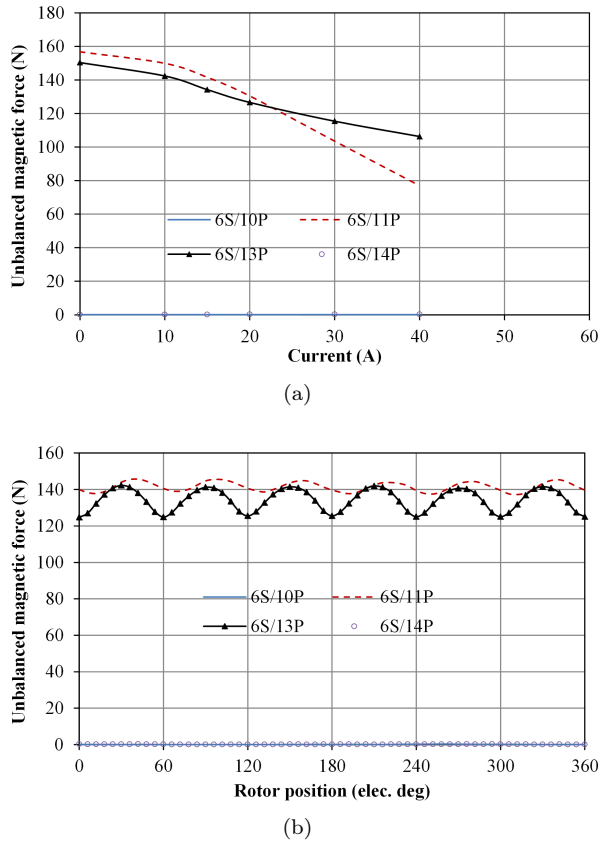$$N_r = N_s \pm k_2 \quad k_2 = 1, 2, ..., \qquad (2)$$

(a)

(b)

Fig. 3: Comparison of Unbalanced magnetic force (UMF) at 400 rpm, 15A (a) UMF versus current and (b) UMF versus rotor position.

stator core and θ_s is the angular coordinate along the stator circumference [23].

$$n = \frac{LCM\,(2p, N_r)}{N_r}, \qquad (6)$$

where LCM is the lowest common multiple between $2p$ and rotor poles, $2p$ is the number of permanent magnet (PM) poles and N_r is the rotor poles [24]. The LCM value between the slot number and rotor pole number of a given electrical machine would really influence the resulting cogging torque value of the machine [18].

Further, the predicted torque ripple (T_r) is calculated using Eq. (7). The applied machine parameters are listed in Tab. 1.

$$T_r = \frac{T_{\max} - T_{\min}}{T_{avg}} \times 100\%, \qquad (7)$$

where: $T_{\max}$, $T_{\min}$ and T_{avg} are the maximum, minimum and average torque, respectively [25].

3. Unbalanced Magnetic Force

Unbalanced magnetic force (UMF) on the rotor is not a desirable machine attribute, since this could lead to

destruction of the permanent magnets (PMs), mainly for the rotor mounted-magnets, and usually at high operating speed, as pointed out in [26]. Therefore, impact of UMF on the rotor of the analyzed machine topologies in this current study is estimated and compared in this Section, using Maxwell Stress Tensor (MST) approach of the adopted finite element analysis (FEA) software. Fig. 3 shows that the resulting unbalanced magnetic force (UMF) on the rotor would depend on the supplied current as well as on the relative angular positions of the rotor. Meanwhile, the largest magnetic force is realized from the machine types that have odd number of rotor poles, whereas its counterparts that are equipped with even number of poles have negligible amount of unbalanced magnetic force. This large amount of UMF is due to the influence of the rotor and stator pole permutations of the analyzed machine type, as proved in [27]. Similarly, the vertical and horizontal components of magnetic forces presented in Fig. 4, also reveal that these forces would have varying effects on the rotor, as seen from their different outlines and magnitudes. More so, it is reconfirmed that the UMF magnitude is dependent on the applied load current. Moreover, the highest amount of UMF would be experienced by the 6S/11P machine type, and then the 6S/13P machine category, under rated speed and current conditions; while the least values of UMF is obtained in the 6S/10P and 6S/14P machine configurations.

Three-dimensional (3D) plots of average unbalanced magnetic force on the rotor as a function of both speed and electric load are displayed in Fig. 5. It is observed that the resulting UMF on the rotors of 6S/11P and 6S/13P increases with increasing electric load current. Nevertheless, the UMF variations with varying rotational speed are fairly constant, as shown in Figs. 5(b) and (c). Although, the 6S/10P and 6S/14P have zigzag variation trends with the current and speed; however, its UMF magnitudes are considerably low compared to that of 6S/11P and 6S/13P machine topologies. The static torque results at different current ratings are shown in Fig. 6. It could be inferred that the resulting static torques in the 6S/11P and 6S/13P machine categories are symmetrical about the rotor angular positions, while its 6S/10P and 6S/14P equivalents are asymmetrical; possibly, due to huge harmonic effects of the later. More so, the magnitudes of the resulting static torque are functions of the supplied currents; the higher the applied current, then, the larger its resultant static torque value. Similarly, it is shown in Fig. 7 that the static torque amplitudes of the compared machine types are basically independent of the machine's rotational speed.
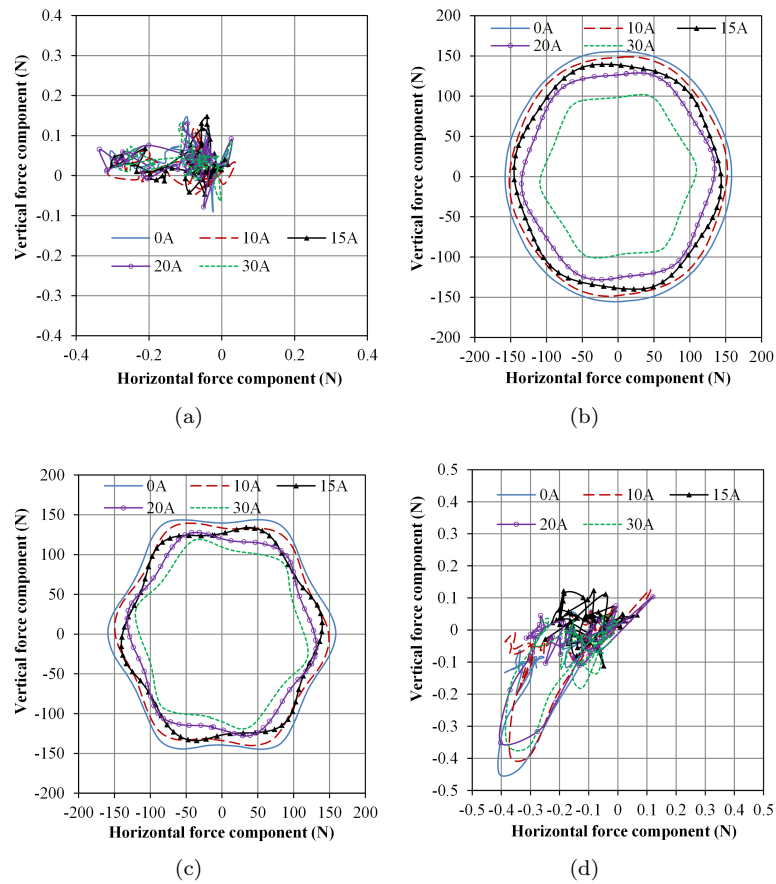
(a)

(b)

(c)

(d)

Fig. 4: Comparison of unbalanced magnetic force at different current levels (a) 6S/10P, (b) 6S/11P, (c) 6S/13P and (d) 6S/14P.
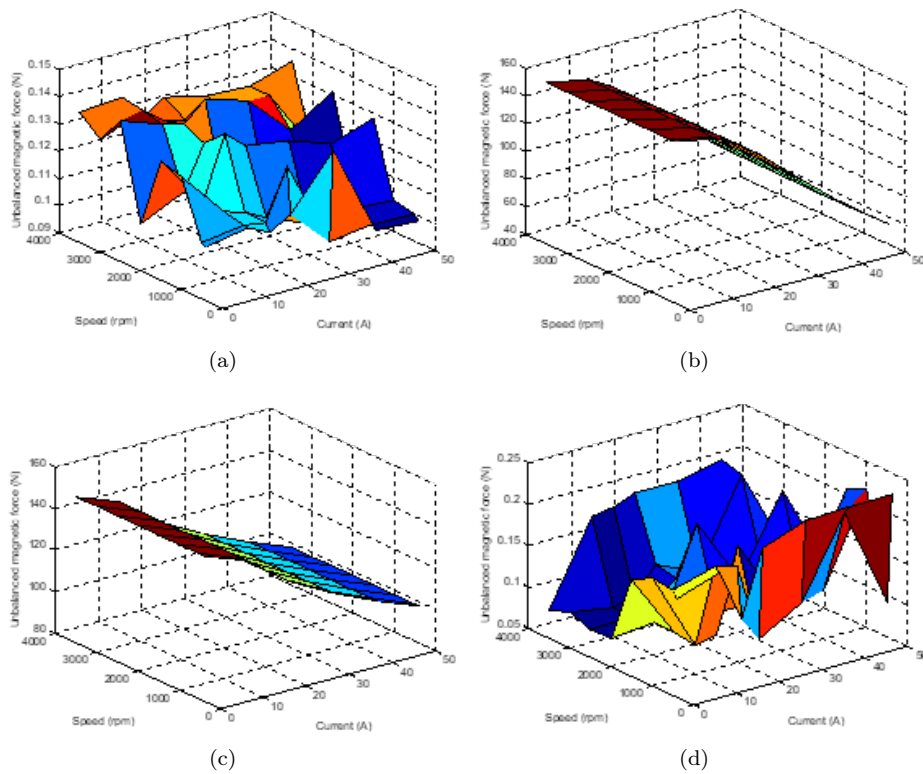

(a)

(b)

(c)

(d)

Fig. 5: Three-dimensional plots of average UMF at different current and speed (a) 6S/10P, (b) 6S/11P, (c) 6S/13P and (d) 6S/14P.

(a)

(b)
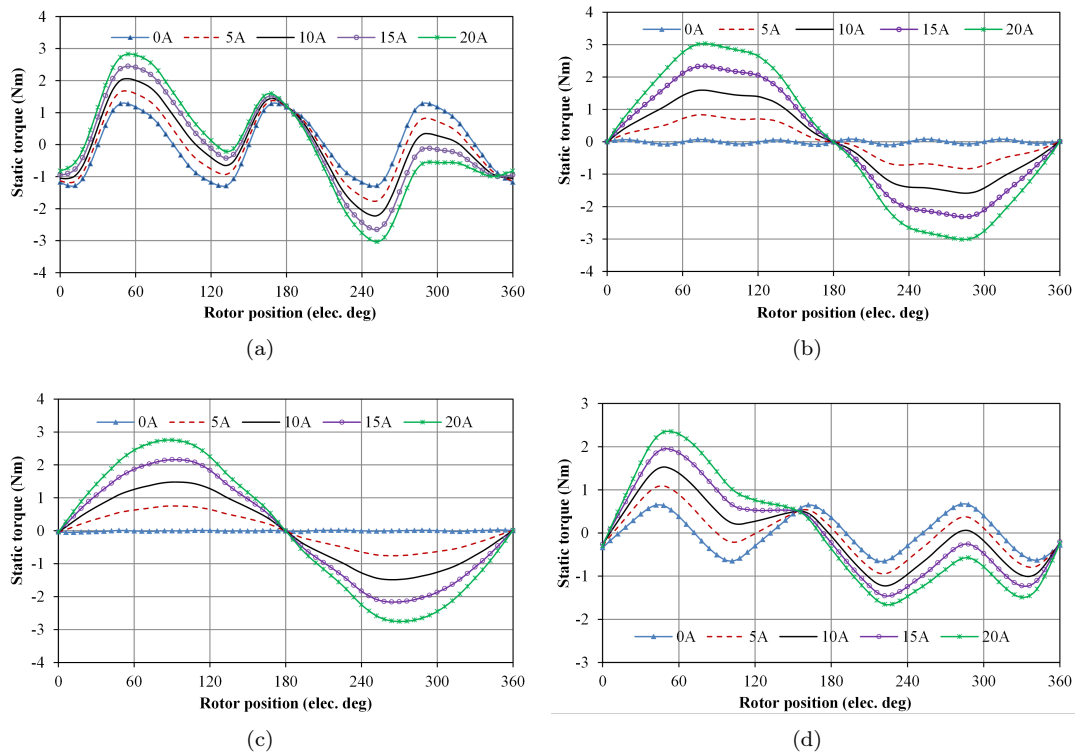
(c)

(d)

Fig. 6: Comparison of static torque, -IA/2=IB=IC (a) 6S/10P, (b) 6S/11P, and (c) 6S/13P and (d) 6S/14P.
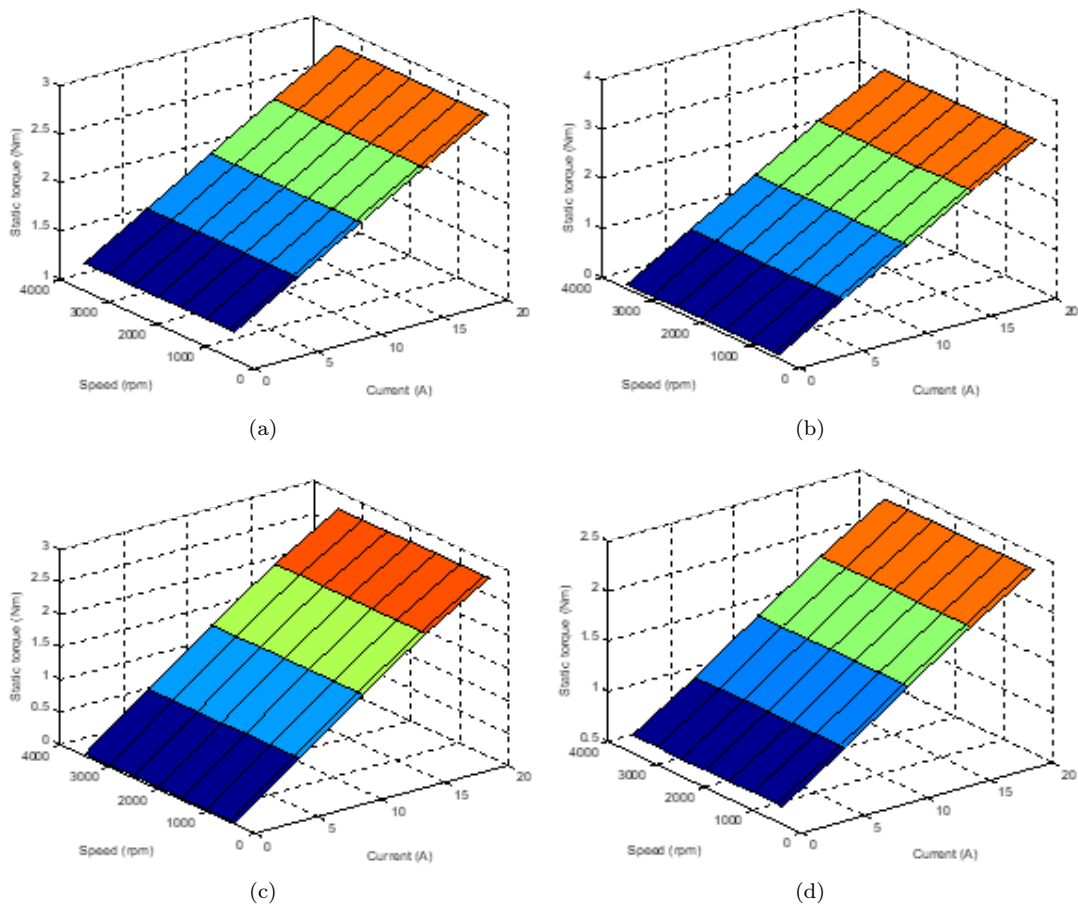

(a)

(b)

(c)

(d)

Fig. 7: Three-dimensional plots of static torque at different current and speed (a) 6S/10P, (b) 6S/11P, (c) 6S/13P and (d) 6S/14P.

Tab. 1: Distribution of the types by rank.

Items	Values			
Inner stator teeth number	6			
Outer stator teeth number	6			
Rotor pole number	10	11	13	14
Average torque (Nm), at rated current and speed	1.37	2.33	2.16	1.27
Air-gap length (mm)	0.5			
Axial length (mm)	25			
Machine diameter (mm)	90			
Stacking factor	0.6			
Rated speed (rpm)	400			
Rated current (A)	15			
Steel material	M330-35A			
Coil material	Copper			
Grade of magnet	N35SH			
Coils per phase	2			
Total number of turns per phase	72			
Magnet remanence (T)	1.2			
Coercive force, H (kA/m)	-909			

4. Total Harmonic Distortion, Torque Ripple and Cogging Torque

The total harmonic distortion (THD) of the voltage variation is depicted in Fig. 8(a). It is obvious that the machine types having even number of rotor poles, exhibit higher amount of THD; likely, due to its high accumulation of harmonic elements. More so, the relationship between the generated THD and supplied load in such machines are fairly linear. Hence, the higher the applied load current, then, the larger its resulting THD value, and vice-versa. Further, the variation of torque ripple with the changing load current is shown in Fig. 8(b). Again, it is observed that the torque ripples are considerably larger in the machines that are furnished with even number of poles, compared to the ones that have odd number of poles. Moreover, an inverse relationship exists between the supplied current and the resulting torque ripple values.

The variations of the THD and torque ripple are nearly constant with changing rotational speed, as depicted in Figs. 9 and 10, respectively. Meanwhile, the torque ripple values of the investigated machines have approximately inverse relationship with the supplied electric load, as well as a fairly constant relationship with the machine's varying speed.

Furthermore, the radial air gap flux densities of the investigated machine types with their resulting harmonic spectra are compared in Fig. 11. It is shown that the produced flux densities are symmetrically and uniformly distributed over the considered rotor angular positions and hence, over the simulated electric period. It is worth noting that the 6S/11P machine type generated the largest air gap flux density; and this invariably would give rise to its other competitive machine qualities, like the output torque and power. More so, the
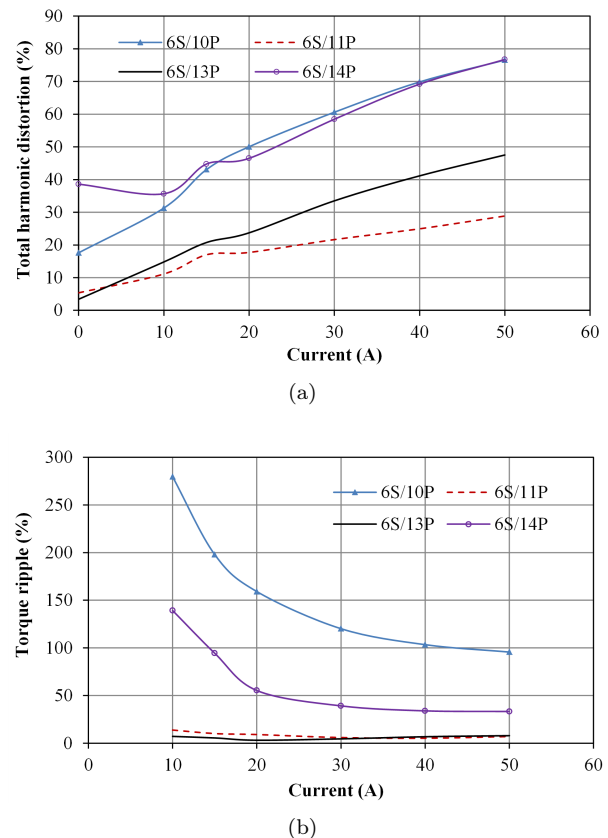

(a)

(b)

Fig. 8: Torque ripple and total harmonic distortion at 400 rpm (a) THD versus current and (b) Torque ripple versus current.
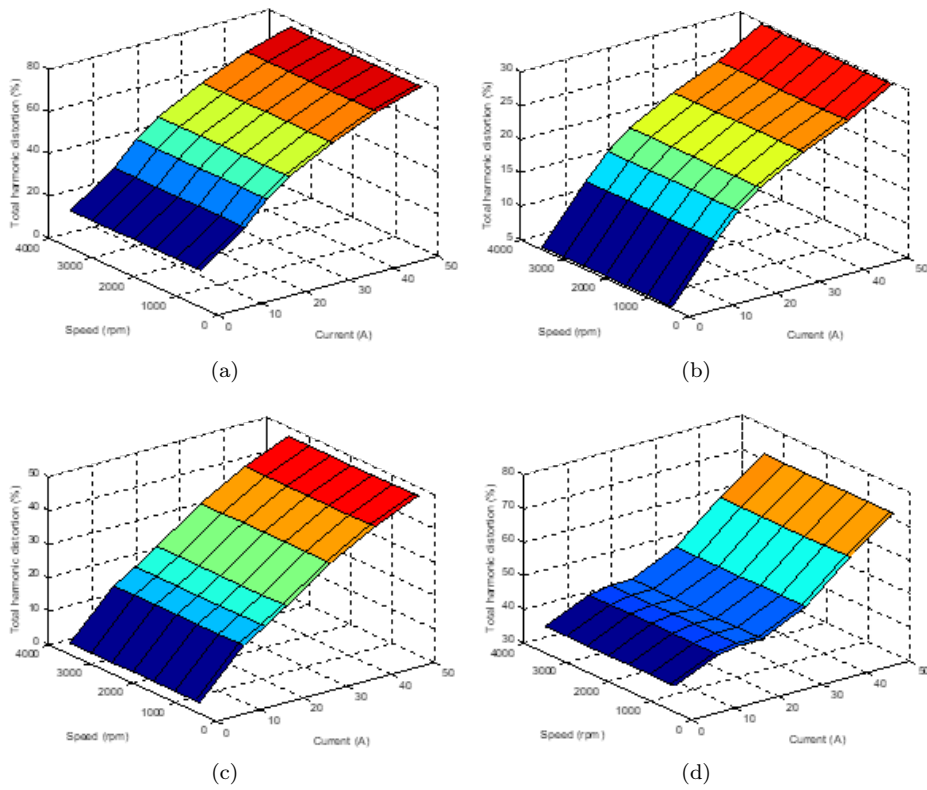
Fig. 9: Three-dimensional plots of THD at different current and speed (a) 6S/10P, (b) 6S/11P, and (c) 6S/13P and (d) 6S/14P.
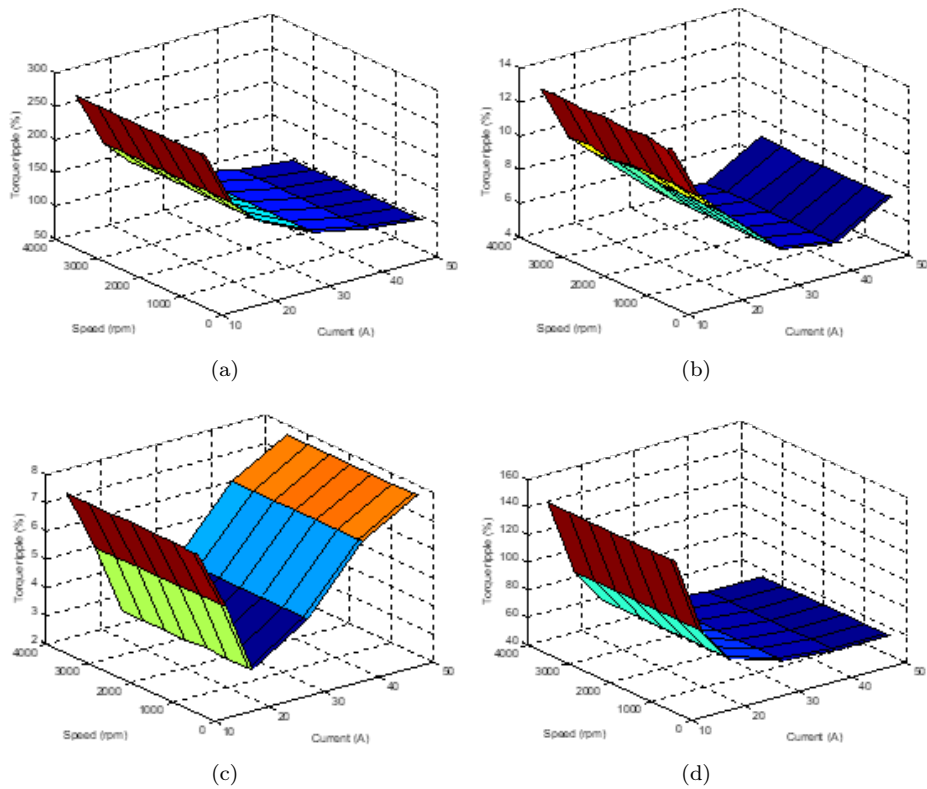

Fig. 10: Three-dimensional plots of torque ripple at different current and speed (a) 6S/10P, (b) 6S/11P, and (c) 6S/13P and (d) 6S/14P.
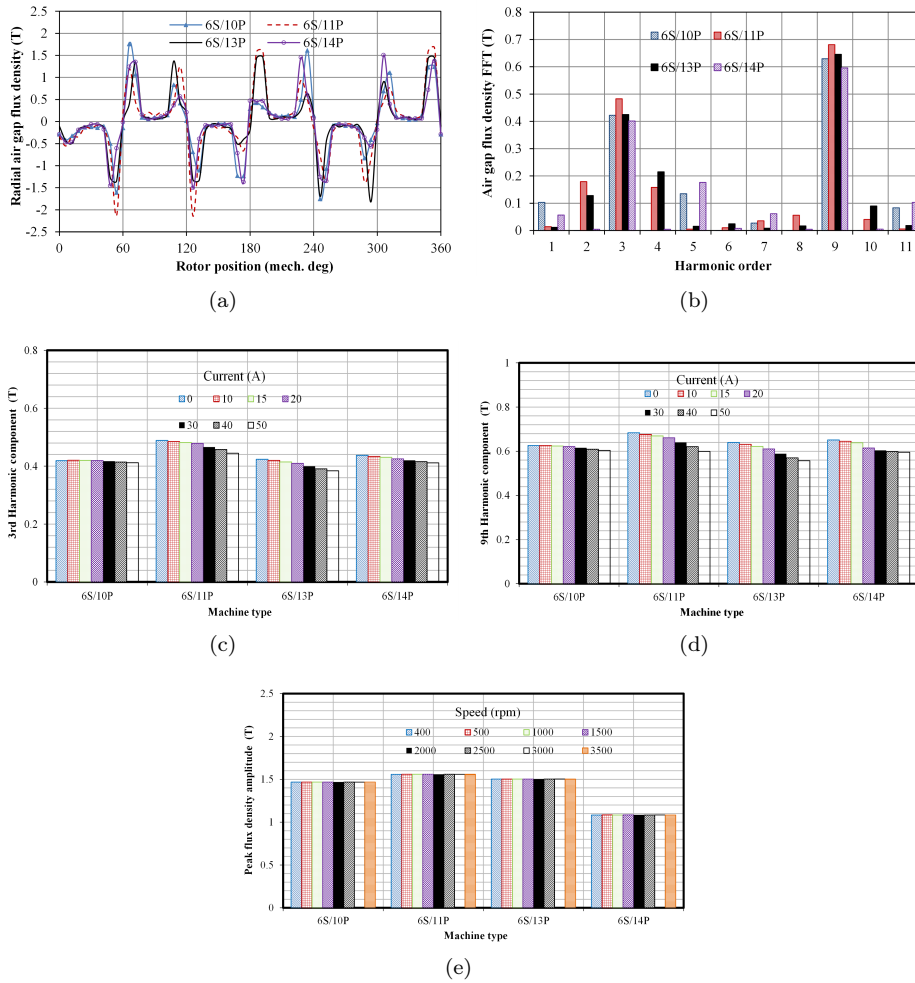
(a)

(b)

(c)

(d)

(e)

Fig. 11: Comparison of the air gap flux density (a) Waveforms on no-load, 400 rpm (b) Fast Fourier Transform (FFT) on no-load, 400 rpm (c) Third (3rd) order harmonics (d) Ninth (9th) order harmonics and (e) Peak flux density at different speed.
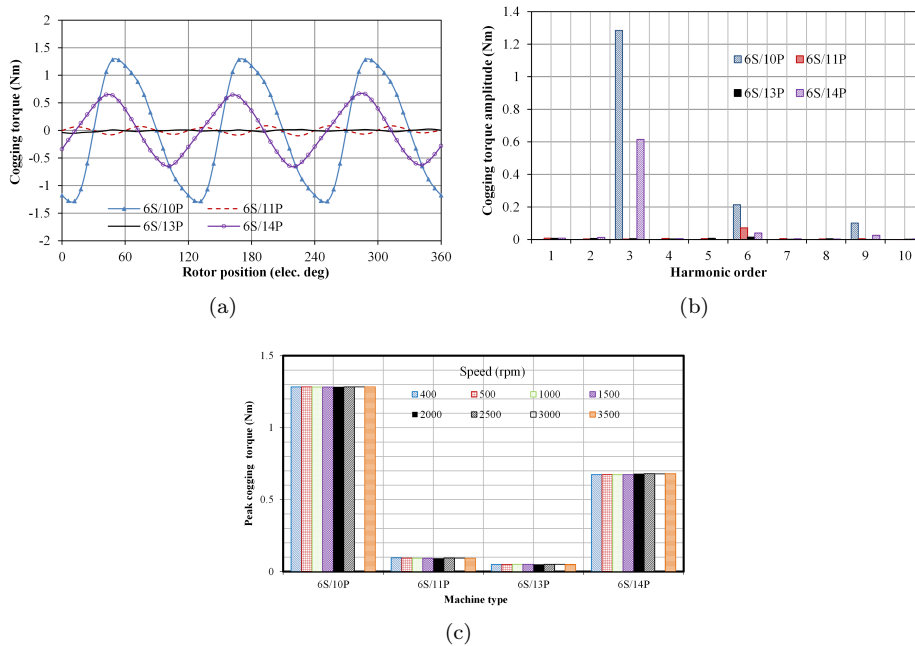

(a)

(b)

(c)

Fig. 12: Cogging torque comparison at 400 rpm (a) Waveforms (b) FFT spectra and (c) Peak cogging at different speed.
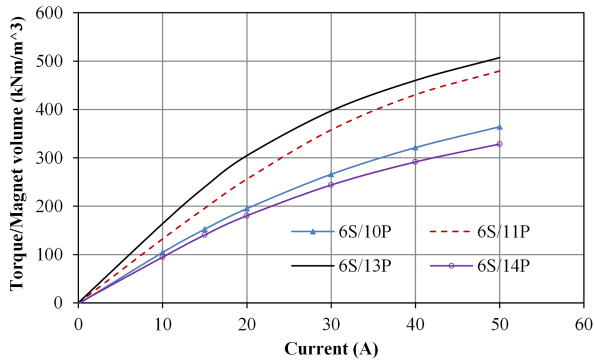
Fig. 13: Comparison of torque per permanent magnet volume.

compared machine types have many useful flux density harmonic orders, as shown in Fig. 11(b). There is abundant useful air gap harmonics in flux-switching permanent magnet (FSPM) machines, as presented in [28]. The dominant flux density harmonic elements of the compared machine types are the 9th and 3rd components, as shown in Fig. 11(b). These dominant harmonic element occurrence is in-line with the obtained results presented in [29] of a typical single stator FSPM machine. Thus, the 3rd and 9th harmonic elements shown in Figs. 11(c) and (d) reveal that the largest fast Fourier transform amplitude of air gap flux density is obtainable on no-load condition, likely, due to the influence of armature reaction. The effect of armature reaction is usually intensified when the machine is electromagnetically saturated. Further, it is obvious from Fig. 11(e) that the maximum air gap flux densities of the analyzed machines are independent of the machine's rotational speed.

Fig. 12(a) shows the cogging torque outlines of the compared machines. The cogging torque amplitudes of 6S/10P and 6S/14P machine configurations are larger than those of its equivalent 6S/11P and 6S/13P machines. This is because; the cogging or no-load torque of a given permanent magnet is customarily related to its torque ripple magnitude. Nevertheless, the cogging torque amplitude of a typical flux-switching machine could be considerably reduced by appropriate modification of its rotor pole structure, as noted in [30]. More so, the machine types having even number of poles have one-half the number of cogging cycles compared to the ones that have odd number of poles. This is in agreement with the mathematical expression of Eq. (6). Hence, the largest amount of cogging torque is obtained in the third (3rd) and sixth (6th) orders, in the two different classes of machine i.e. even rotor pole (6S/10P and 6S/14P) and odd rotor pole (6S/11P and 6S/13P) machine categories, respectively; as depicted in Fig. 12(b). Fig. 12(c) shows that the cogging torque amplitude of the investigated machine types is not dependent upon the machine's rotational speed.

Although, the analyzed 11-pole machine type (6S/11P) has the most promising electromagnetic performances; the 13-pole (6S/13P) machine would produce the best average torque, if all the machine categories are simulated using the same volume of magnetic material, as shown in Fig. 13. The worst amongst all the compared machines with regard to output performance(s) is the 14-pole machine type (6S/14P). Additionally, the produced torque per magnet volume is essentially independent of the rotor speed, as shown in Fig. 14.

5. Conclusion

It is established that most of the undesirable machine characteristics are exhibited by the machine types that are equipped with even number of rotor poles i.e. 6S/10P and 6S/14P machine categories; although, rotor of the machine types that have odd number of poles i.e. the 6S/11P and 6S/13P machine types would experience larger amount of unbalanced magnetic force, which is a demerit. It is also shown that compared machine types have many useable flux density harmonics. Additionally, the 11- and 13-pole machine types also have higher amounts of air gap flux densities, which is desirable for larger electromotive force and output torque generations. The static torque waveforms of the compared machine that have even number of rotor poles are asymmetric over the simulated rotor positions, unlike its counterparts that have odd number of rotor poles. Most of the investigated performance indices are independent of the machine's rotational speed. Above all, the machines that have 13-pole and 11-pole have the best torque per used magnet material; thus the most cost-effective machine to produce amongst all the compared machine configurations. The worst case scenario, in terms of electromagnetic output performance is exhibited by the 6S/14P machine type.

Author Contributions

References

[1] MAGNUSSEN, F., and H. LENDENMANN. Parasitic effects in PM machines with concentrated windings. *IEEE Transactions on Industry Ap-*
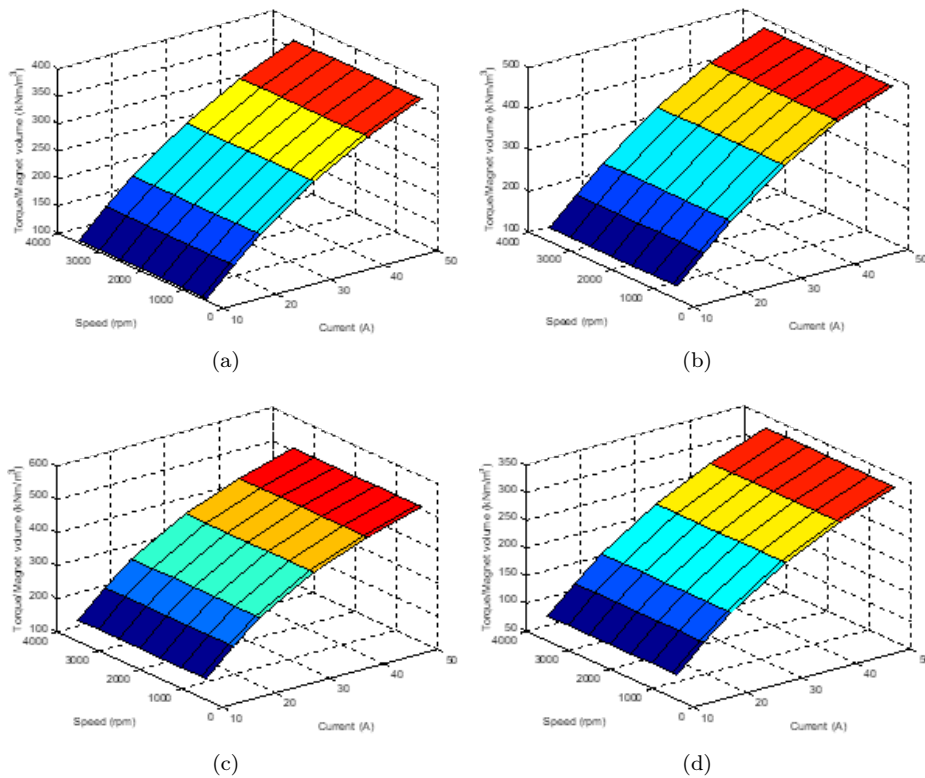
Fig. 14: Three-dimensional plots of average torque per magnet volume at different current and speed (a) 6S/10P, (b) 6S/11P, (c) 6S/13P and (d) 6S/14P.

plications. 2007, vol. 43, iss. 5, pp. 1223–1232. DOI: 10.1109/TIA.2007.904400.

[2] HUANG, C., H. YUAN, W. CAO and Y. WU. Multi-objective optimization design of ERSRM with asymmetric stator poles. *2023, Progress in Electromagnetics Research C*, vol. 129, iss. 2, 257–271. DOI: 10.2528/PIERC22120218.

[3] QI, J., Z. ZHU, L. YAN, G.W. JEWELL, C. GAN, Y. REN, S. BROCKWAY and C. HILTON. Influence of armature reaction on electromagnetic performance and pole shaping effect in consequent pole PM machines. *Energies*. 2023, vol. 16, iss. R, pp. 1982. DOI: 10.3390/en16041982.

[4] DORRELL, D.G., M.F. HSIEH and Y.G. GUO. Unbalanced magnet pull in large brushless rare-earth permanent magnet motors with rotor eccentricity. *IEEE Transactions on Magnetics*. 2009, vol. 45, iss. 10, pp. 4586–4589. DOI: 10.1109/TMAG.2009.2022338.

[5] TORABI, M., and Y.A. BEROMI. An effective Hilbert–Huang transform-based approach for dynamic eccentricity fault diagnosis in double-rotor double-sided stator structure axial flux permanent magnet generator under various load and speed conditions. *Turkish Journal of Electrical Engi-*

neering and Computer Sciences. 2023, vol. 31, iss. 1, pp. 53–76. DOI: 10.55730/1300-0632.3971.

[6] Song, J.Y., K.J. Kang, C.H. Kang and G.H. Jang. Cogging torque and unbalanced magnetic pull due to simultaneous existence of dynamic and static eccentricities and uneven magnetization in permanent magnet motors. *IEEE Transactions on Magnetics*. 2017, vol. 53, iss. 3, pp. 1–9. DOI: 10.1109/TMAG.2016.2628098.

[7] DORRELL, D.G., M. POPESCU and D.M. IONEL. Unbalanced magnetic pull due to asymmetry and low-level static rotor eccentricity in fractional-slot brushless permanent-magnet motors with surface-magnet and consequent-pole rotors. *IEEE Transactions on Magnetics*. 2010, vol. 46, iss. 7, pp. 2675–2685. DOI: 10.1109/TMAG.2010.2044582.

[8] DORRELL, D.G., J.K.H. SHEK and M.F. HSIEH. The development of an indexing method for the comparison of unbalanced magnetic pull in electrical machines. *IEEE Transactions on Industry Applications*. 2016, vol. 52, iss. 1, pp. 145–153. DOI: 10.1109/TIA.2015.2466554.

[9] ZHU, Z.Q., L.J. WU and M.L.M. JAMIL. Influence of pole and slot number combinations on cogging torque in permanent-magnet

machines with static and rotating eccentricities. *IEEE Transactions on Industry Applications.* 2014, vol. 50, iss. 5, pp. 3265–3277. DOI: 10.1109/TIA.2014.2308363.

[10] ZHU, Z.Q., L.J. WU and M.L.M. JAMIL. Influence of pole and slot number combinations on cogging torque in permanent-magnet machines with static and rotating eccentricities. *IEEE Transactions on Industry Applications.* 2014, vol. 50, iss. 5, pp. 3265–3277. DOI: 10.1109/TEC.2015.2436065.

[11] WASHINGTON, J.G., G.J. ATKINSON and N.J. BAKER. Reduction of cogging torque and EMF harmonics in modulated pole machines. *IEEE Transactions on Energy Conversion.* 2016, vol. 31, iss. 2, pp. 759–768. DOI: 10.1109/TEC.2016.2520200.

[12] ZHU, X., W. HUA and G. ZHANG. Analysis and reduction of cogging torque for flux-switching permanent magnet machines. *IEEE Transactions on Industry Applications.* 2019, vol. 55, iss. 6, pp. 5854–5864. DOI: 10.1109/TIA.2019.2938721.

[13] BRAMERDORFER, G. Computationally efficient tolerance analysis of the cogging torque of brushless PMSMs. *IEEE Transactions on Industry Applications.* 2017, vol. 53, iss. 4, pp. 3387–3393. DOI: 10.1109/TIA.2017.2682797.

[14] SONG, Z., Y. YU, F. CHAI and Y. TANG. Radial force and vibration calculation for modular permanent magnet synchronous machine with symmetrical and asymmetrical open-circuit faults. *IEEE Transactions on Magnetics.* 2018, vol. 54, iss. 11, pp. 1–5. DOI: 10.1109/TMAG.2018.2848724.

[15] CHOO, Y., C. KIM, G. YUN and C. LEE. Investigation of torque ripple in an induction motor with respect to slot number combinations. *Journal of Magnetics.* 2022, vol. 27, iss. 1, pp. 18–27. DOI: 10.4283/JMAG.2022.27.1.018.

[16] PARK, E.J., and Y.J. Kim. Torque ripple according to the number of permanent magnet poles of magnetic gear. *Journal of Magnetics.* 2022, vol. 27, iss. 1, pp. 51–55. DOI: 10.4283/JMAG.2022.27.1.051.

[17] WANG, H., and S. DING. Design and analysis of new dual-stator field modulation machines with multiple magnetic excitations. *IEEE Transactions on Magnetics.* 2021, vol. 57, iss. 2, pp. 1–6. DOI: 10.1109/TMAG.2020.3005462.

[18] CHEN, Z., N. XING, H. MA, Z. LI, J. LI and C. FAN. Armature MMF and electromagnetic performance analysis of dual three-phase 10-pole/24-slot permanent magnet synchronous machine.

Archives of Electrical Engineering. vol. 72, iss. 1, pp. 189–210. DOI: 10.24425/aee.2023.143697.

[19] CHEN, J.T., Z.Q. ZHU, S. IWASAKI and R.P. DEODHAR. A novel E-core switched-flux PM brushless AC machine. *IEEE Transactions on Industry Applications.* 2011, vol. 47, iss. 3, pp. 1273–1282. DOI: 10.1109/TIA.2011.2126543.

[20] CHEN, J.T., and Z.Q. ZHU. Winding configurations and optimal stator and rotor pole combination of flux-switching PM brushless AC machines. *IEEE Transactions on Energy Conversion.* 2010, vol. 25, iss. 2, pp. 293–302. DOI: 10.1109/TEC.2009.2032633.

[21] AWAH, C.C. A new topology of double-stator permanent magnet machine equipped with AC windings on both stators. *Archives of Electrical Engineering.* 2022, vol. 71, iss. 2, pp. 283–296. DOI: 10.24425/aee.2022.140711.

[22] AWAH, C.C., O.I. OKORO, E. CHIKUNI. Cogging torque and torque ripple analysis of permanent magnet flux-switching machine having two stators. *Archives of Electrical Engineering.* 2019, vol. 68, iss. 1, pp. 115–133. DOI: 10.24425/aee.2019.125984.

[23] ŽARKO, D., D. BAN, I. VAZDAR and V. JARIC. Calculation of unbalanced magnetic pull in a salient-pole synchronous generator using finite-element method and measured shaft orbit. *IEEE Transactions on Industrial Electronics.* 2012, vol. 59, iss. 6, pp. 2536–2549. DOI: 10.1109/TIE.2011.2160515.

[24] EVANS, D.J., and Z.Q. ZHU. Novel partitioned stator switched flux permanent magnet machines. *IEEE Transactions on Magnetics.* 2015, vol. 51, iss. 1, pp. 1–14. DOI: 10.1109/TMAG.2014.2342196.

[25] LIU, X., W. WANG, S. ZHU, Y. GAO and J. FU. Design and optimization of a reverse salient pole flux controlled permanent magnet motor. *Progress in Electromagnetics Research C.* 2023, vol. 129, iss. 2, pp. 127–141. DOI: 10.2528/PIERC22112901.

[26] DU, G., W. XU, J. ZHU and N. HUANG. Effects of design parameters on the multiphysics performance of high-speed permanent magnet machines. *IEEE Transactions on Industrial Electronics.* 2020, vol. 67, iss. 5, pp. 3472–3483. DOI: 10.1109/TIE.2019.2922933.

[27] MA, J., and Z.Q. ZHU. Mitigation of unbalanced magnetic force in a PM machine

with asymmetric winding by inserting auxiliary slots. *IEEE Transactions on Industry Applications.* 2018, vol. 54, iss. 5, pp. 4133–4146. DOI: 10.1109/TIA.2018.2829879.

[28] SHI, Y., L. JIAN, J. WEI, Z. SHAO, W. LI, and C.C. CHAN. A new perspective on the operating principle of flux-switching permanent-magnet machines. *IEEE Transactions on Industrial Electronics.* 2016, vol. 63, iss. 3, pp. 1425–1437. DOI: 10.1109/TIE.2015.2492940.

[29] EGUREN, I., G. ALMANDOZ, A. EGEA, X. BADIOLA and A. URDANGARIN. Understanding switched-flux machines: A MMF-permeance model and magnetic equivalent circuit approach. *IEEE Access.* 2022, vol. 10, pp. 69096–928. DOI: 10.1109/ACCESS.2022.3140977.

[30] LI, Y., D. BOBBA and B. SARLIOGLU. A novel 6/4 flux-switching permanent magnet machine designed for high-speed operations. *IEEE Transactions on Magnetics.* 2016, vol. 52, iss. 8, pp. 8107109. DOI: 10.1109/TMAG.2016.2547366.

About Authors

Chukwuemeka AWAH (corresponding author) was born in Nsukka, Nigeria. He received the B.Eng., and M.Eng. degrees in Electrical Engineering, from the University of Nigeria, Nsukka in 2005 and 2009, respectively, and the PhD degree in 2016 from the department of Electronic and Electrical Engineering, the University of Sheffield, UK, under the Commonwealth Scholarship Award Scheme. Dr. Awah is a Senior Member of the Institute of Electrical and Electronics Engineers (SMIEEE), USA; and an active reviewer of many reputable journals: IEEE and other journals. He is also a member of the Nigerian Society of Engineers. Awah is registered with the Council for the Regulation of Engineering in Nigeria. He is a Faculty Member in the College of Engineering and Engineering Technology of Michael Okpara University of Agriculture, Umudike, Nigeria. He has published widely in reputable local and international journals. His main research interests include modelling, design and analysis of electrical machines.

Stephen OTI was born in Nsukka, Nigeria. He received a B.Eng. (Electrical Engineering), an M.Eng. (Electrical Power Devices) and a Ph.D (Electrical Power Devices) degrees, all of the University of Nigeria in 1998, 2006 and 2014, respectively. He is currently a Reader (Associate Professor) in the department of Electrical Engineering, the University of Nigeria, Nsukka. He is a member of Nigerian Society of Engineers (NSE). He is a member of Nigerian Institute of Electrical and Electronic Engineering (NIEEE) and he is also a registered member of Council for the Regulation of Engineering in Nigeria (COREN). He has several research articles published both in local and international journals. His research areas include machine modelling, thermal modelling, power and energy systems modelling.

Ifeanyi NNABUENYI was born in Agulu, Nigeria. He received the B. Eng degree in Electrical and Electronics from the department of Electrical, Electronics and Computer Engineering, Nnamdi Azikiwe University, Awka, Nigeria in 2004. He received the M.Sc degree in Applied Instrumentation and Control from Glasgow Caledonian University, Scotland, United Kingdom in 2011.